Van Gogh: A New Drosophila Tissue Polarity Gene

Job Taylor, Natasha Abramova,[1] Jeannette Charlton and Paul N. Adler

Biology Department and Cancer Center, University of Virginia, Charlottesville, Virginia 22903

ABSTRACT

Mutations in the *Van Gogh* gene result in the altered polarity of adult Drosophila cuticular structures. On the wing, *Van Gogh* mutations cause an altered polarity pattern that is typical of mutations that inactivate the *frizzled* signaling/signal transduction pathway. The phenotype however, differs from those seen previously, as the number of wing cells forming more than one hair is intermediate between that seen previously for typical *frizzled*-like or *inturned*-like mutations. Consistent with *Van Gogh* being involved in the function of the *frizzled* signaling/signal transduction pathway, *Van Gogh* mutations show strong interactions with mutations in *frizzled* and *prickle*. Mitotic clones of *Van Gogh* display domineering cell nonautonomy. In contrast to *frizzled* clones, *Van Gogh* clones alter the polarity of cells proximal (and in part anterior and posterior) but not distal to the clone. In further contrast to *frizzled* clones, *Van Gogh* clones cause neighboring wild-type hairs to point away from rather than toward the clone. This anti-*frizzled* type of domineering nonautonomy and the strong genetic interactions seen between *frizzled* and *Van Gogh* suggested the possibility that *Van Gogh* was required for the noncell autonomous function of *frizzled*. As a test of this possibility we induced *frizzled* clones in a *Van Gogh* mutant background and *Van Gogh* clones in a *frizzled* mutant background. In both cases the domineering nonautonomy was suppressed consistent with *Van Gogh* being essential for *frizzled* signaling.

THE cuticular surface of Drosophila is decorated with large numbers of polarized structures such as hairs, bristles and ommatidia. In any body region these structures are aligned in parallel, giving the region a "tissue polarity." In recent years the genetic basis for the development of tissue polarity in the wing, eye and abdomen has been studied in some depth (Adler 1992; Gubb 1993; Zheng *et al.* 1995; Kopp and Duncan 1997; Struhl *et al.* 1997; Strutt *et al.* 1997). We have used the wing as a model system because of the simple, flat structure of the tissue and the ease of examining the array of distally pointing hairs that decorate it. Almost all pupal wing cells form a single microvillus-like prehair that gives rise to the adult cuticular hair (Wong and Adler 1993). The prehairs are formed at the cell periphery in the vicinity of the distal-most region of the cell and extend distally as they grow, leading to the distally pointing adult cuticular hair (Wong and Adler 1993). Hair polarity is tightly correlated with the subcellular location for prehair initiation. Mutations that cause nondistal polarity appear to do so via altering the subcellular location for prehair initiation (Wong and Adler 1993). Previous studies have suggested that most, if not all, known tissue polarity genes are members of the *frizzled* (*fz*) signaling/signal transduction pathway that controls hair polarity by regulating the subcellular location for prehair initiation (Wong and Adler 1993). This pathway contains both cell autonomously and cell nonautonomously acting genes (Vinson and Adler 1987; Wong and Adler 1993). Several aspects of the tissue polarity phenotype have been used to characterize tissue polarity mutants and genes. The cellular phenotype (number of hairs per cell and the subcellular location for prehair initiation) allows mutants to be placed into three phenotypic groups that also represent epistasis groups [the *frizzled* (*fz*)-like genes, the *inturned* (*in*)-like genes and the *multiple wing hair* (*mwh*) gene; Wong and Adler 1993]. An alternative way to classify tissue polarity genes is based on the abnormal mutant wing polarity patterns that are stereotypic for individual genes (Gubb and Garcia-Bellido 1982; Wong and Adler 1993). Most tissue polarity mutations result in a similar, albeit not identical, pattern that we refer to as the *fz*/*in*-like polarity pattern. Mutations that inactivate the *fz* signaling/signal transduction pathway result in this pattern. Mutations that alter the anatomical direction of *fz* signaling cause unique and different patterns (Adler *et al.* 1998; R. E. Krasnow and P. N. Adler, unpublished results).

We recently carried out a large mutant screen designed to identify and recover new tissue polarity mutations. In addition to recovering recessive mutations as the screen was designed to do, we also identified and recovered a number of dominant tissue polarity mutations. One gene identified in this screen because of a dominant mutant phenotype, *Van Gogh* (*Vang*), is the subject of this paper.

The first *Vang* mutation was identified on the basis of a region of hair swirling in the C′ cell of the wing (this is the region of the wing that lies between the third and fourth veins proximal to the anterior cross vein). Many,

Corresponding author: Paul Adler, Biology Department, University of Virginia, Charlottesville, VA 22903. E-mail: pna@virginia.edu

[1]*Present address:* Biochemistry Department, Health Sciences Center, University of Virginia, Charlottesville, VA 22903.

but not all *Vang* alleles display this dominant phenotype. Homozygous *Vang* mutant wings show a tissue polarity phenotype that in terms of the cellular phenotype falls in between typical *frizzled*-like and *inturned*-like mutant phenotypes (Wong and Adler 1993; Krasnow and Adler 1994), suggesting that this gene might have a unique function in tissue polarity. *Vang* mutations cause a *fz*/*in*-like polarity pattern suggesting that mutations in *Vang* inactivate the *fz* pathway.

We have used the weak dominant phenotype to look for interactions with other tissue polarity genes. The two most compelling were the dominant enhancement of this phenotype by *frizzled* mutations and the dominant suppression of this phenotype by *prickle* (*pk*) mutations. Other genetic interactions were also seen between *Vang* and both *fz* and *pk*, suggesting a close functional relationship between these genes.

Mutations in *fz* are notable for the directional domineering cell nonautonomy shown by most alleles (Vinson and Adler 1987). Cells distal (and in part posterior and anterior) to a *fz* clone show altered hair polarity, with the neighboring wild-type hairs tending to point toward the clone (Adler *et al.* 1997). Marked mitotic clones of two independent *Vang* alleles were generated and found to show a remarkable "anti-*fz*" phenotype. That is, neighboring wild-type cells located proximal (and anterior and posterior) but not distal to the clone showed altered hair polarity. These wild-type hairs tended to point away from the clone—the opposite of what is seen for *fz*. To test if these opposite phenotypes could be because of an interaction between these two genes, we generated *fz* clones in a *Vang* mutant background and *Vang* clones in a *fz* mutant background. In both cases the cell nonautonomy of *fz* and *Vang*, respectively, were substantially suppressed. The data suggest that *Vang* is essential for *fz* intercellular signaling.

MATERIALS AND METHODS

Fly culture and strains: Flies were grown on standard media at 25° (unless stated otherwise). Many mutant- and deficiency-containing stocks were obtained from the stock centers at Indiana University, Bowling Green State University, and Umeå University. Several important deficiency chromosomes were kindly provided by the Konev laboratory. We carried out a large-scale mutant screen that utilizes FLP/FRT technology (Golic and Lindquist 1989; Xu and Rubin 1993) to recover mutations that cause altered hair polarity. The details of this screen will be presented elsewhere (P. N. Adler, J. Charlton and J. Liu, unpublished results). Briefly, FRT-carrying flies were mutagenized with EMS, crossed to *hs-flp;FRT*-carrying flies and clones induced in the F_1 progeny via heat shocking larvae. The adult F_1 flies were anesthetized under CO_2, and one wing was removed without killing the fly. The wing was examined under a compound microscope and flies that had clones with altered hair polarity, number, or morphology were saved and bred to recover the mutation. In these screens we also recovered dominant mutations. The isolation of *Vang* mutations because of their dominant phenotype resulted in the start of the experiments reported here. Additional *Vang* alleles were isolated after EMS or γ-ray mutagenesis by their failure to complement an existing *Vang* allele. The gene was named *Van Gogh* because the swirling wing hair patterns bring to mind the swirling brush strokes this artist used in some of his paintings.

Cytological procedures: To examine the process of hair morphogenesis pupal wings were dissected in PBS + 4% paraformaldehyde, stained with a fluorescent phalloidin (that binds to F-actin; Wong and Adler 1993), and examined by confocal microscopy using a Molecular Dynamics (Sunnyvale, CA) confocal microscope.

Generation of genetic mosaics: Several types of mosaic experiments were carried out. In all we used the FLP/FRT system to generate clones of interest. For example, to determine if *Vang* acted in a cell in an autonomous or nonautonomous fashion we constructed larvae that were *w hsflp; FRT42 Vang*^{A3} *kojak*^{VB13}/*FRT42*. These were heat shocked at 38° for ½ hr to induce the expression of the *hs-flp* gene and recombination at the FRT site. The subsequent clone could be recognized because of being homozygous for the recessive mutation *kojak* (*koj*). This mutation results in some cells forming multiple, split, and shortened hairs and others no hair (*i.e.*, a bald cell). In other experiments we have found that *koj* is cell autonomous. The *koj* alleles used were isolated in our FLP/FRT screen. We used a new hair morphology marker *starburst* (*strb*) to mark *fz* clones (Park *et al.* 1996). In other experiments we also used *pawn* (*pwn*) as a cell marker for *2*R and *flare* (*flr*) as a cell marker for *3*L.

Scoring of mutant wings: Wings from relevant flies were mounted in Euparal (Asco Labs) and examined under bright field microscopy. As part of the analysis we often made drawings of individual wings that showed the abnormal polarity pattern of wing hairs on the dorsal surface of the wing. The pattern shown is of an individual wing; however, at least five other wings of that genotype were examined to insure that the wing drawn was typical for the genotype. In previous studies we have used several different quantitative assays to characterize tissue polarity phenotypes (*e.g.*, number of multiple hair cells). These are described in detail elsewhere (Wong and Adler 1993; Krasnow and Adler 1994; Adler *et al.* 1994; Park *et al.* 1996).

RESULTS

Isolation of *Vang*: Our two original *Vang* alleles were recovered because of a dominant phenotype—a swirl in the wing hair pattern in the C′ region of the wing (this is the region that lies between the third and fourth veins proximal to the proximal cross vein; Figure 1B—compare to the wild-type pattern in this region; Figure 1A). Eight additional alleles were isolated via screening for a lack of complementation with the original allele. Flies homozygous for *Vang* alleles show a tissue polarity bristle phenotype on the wing, thorax, legs and abdomen. On the abdomen, bristles point almost orthogonally to the midline instead of posteriorly. The tarsus joints are often duplicated as is typical for tissue polarity mutants (Held *et al.* 1986). The flies also have rough eyes, which we suspect is because of a tissue polarity effect (Zheng *et al.* 1995). *Vang* was mapped to meiotic map position 60 on *2*R. It was mapped to cytological interval 45AB on the basis of being uncovered by *Df(2R)NP4* (44F; 45B) and *Df(2R)w45-30N* (45A; 45E).

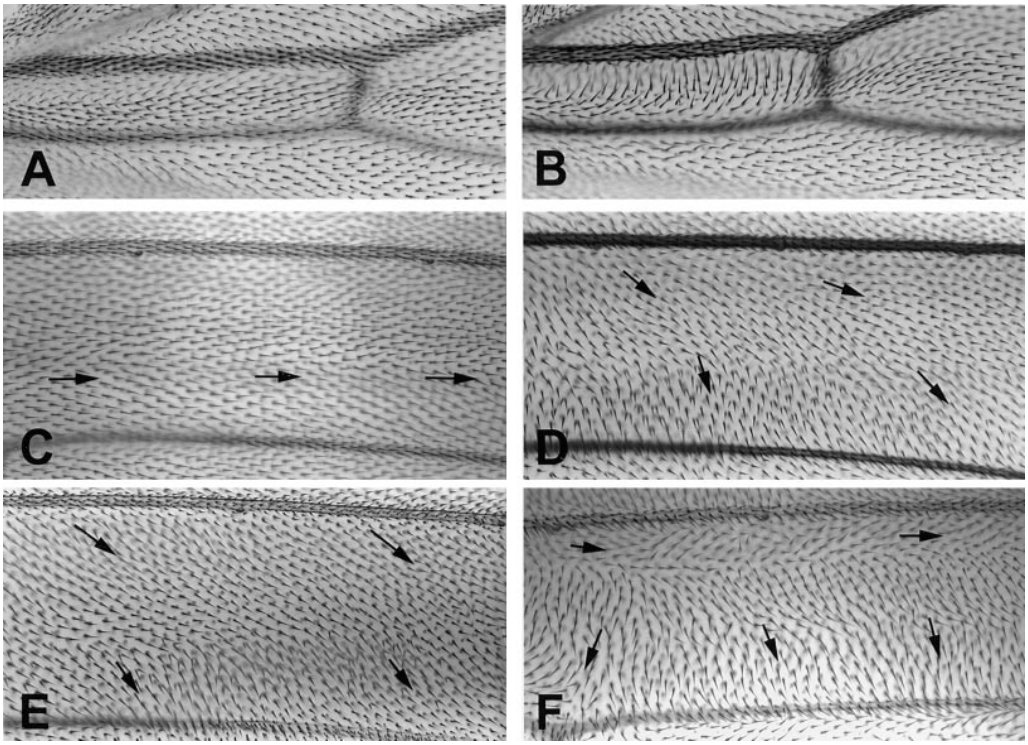

Figure 1.—All micrographs are of the dorsal surface of the wing. A shows the C′ region of a wild-type Oregon R wing. B shows the C′ region of a *Vang*^{TBS42}/+ wing. Note the swirling hairs in this region. C–F show the middle part of the C cell (distal to the posterior cross vein) in: (C) Oregon R, (D) *Vang*^{TBS42}/*Vang*^{TBS42}, (E) *Vang*^{A3}/*Vang*^{A3}, and (F) *Vang*^{4014}/*Vang*^{4014} wings. Arrows are in the local direction of polarity. Note that *Vang*^{TBS42}/*Vang*^{TBS42} has a slightly stronger phenotype than *Vang*^{A3}/*Vang*^{A3} and that *Vang*^{4014}/*Vang*^{4014} has the strongest polarity phenotype, but very few multiple hair cells. In all wing figures proximal is to the left and distal to the right.

The presence of either of these deficiencies is simply noted by *Df* in the text.

Several *Vang* alleles, *e.g.*, *Vang*^{TBS42} (see Table 1), showed complete penetrance for the dominant C′ swirl phenotype (Figure 1B). For these alleles (and indeed for all *Vang* alleles that showed the dominant C′ phenotype) the phenotype was stronger in flies raised at 29° than 18°. Deficiencies for the region showed no dominant C′ phenotype at 18° and a weak and incompletely penetrant one at 29°. By this genetic criterion we conclude that *Vang* alleles such as *Vang*^{TBS42} that show complete penetrance for this dominant phenotype have at least some antimorphic character. We further conclude that the temperature sensitivity of the dominant phenotype is not because of temperature-sensitive mutant proteins. Several alleles, such as *Vang*^{A3}, showed a weak and incompletely penetrant dominant C′ phenotype. This was similar to what was seen with deficiencies for the region; hence by this genetic test (and for this phenotype) *Vang*^{A3} appears to be amorphic and it may represent a null allele. Several *Vang* alleles did not show any evidence of a dominant phenotype and are likely hypomorphic alleles.

Phenotypic characterization of *Vang*: Homozygotes for 9 of the 10 Vang alleles showed a similar tissue polarity phenotype that differed only in severity (Figure 1, D–F). Consistent with the suggestion above that *Vang*^{A3} is an amorphic allele, *Vang*^{A3}/*Vang*^{A3} and *Vang*^{A3}/*Df* flies had similar phenotypes. Consistent with the suggestion that *Vang*^{TBS42} is an antimorphic allele, homozygous *Vang*^{TBS42} flies appeared to have a stronger wing phenotype than *Vang*^{TBS42}/*Df* flies. However, for

TABLE 1

***Van Gogh* alleles**

Allele name	Mutagen	Dominant phenotype[a]	Homozygous phenotype[b]
TBS42	EMS	Antimorphic	Antimorphic
A5	Gamma ray	Antimorphic	Hypomorphic
A3	Gamma ray	Amorphic	Amorphic
XG41	EMS	Amorphic	Amorphic
11-3	Gamma ray	Amorphic	Amorphic
14-11	Gamma ray	Antimorphic	Antimorphic
4041	Gamma ray	Hypomorphic	Frizzled-like
Deficiency[c]		Amorphic	

Two *Vang* alleles isolated in our screens and confirmed by complementation tests were lost and are not included in this table.

[a] The dominant C′ phenotype is compared to the phenotype produced by a *Df*. Those alleles that caused a dominant phenotype with stronger expressivity and higher penetrance than the *Df* are scored as antimorphic. Those that appeared similar to a *Df* in causing a phenotype with weak expressivity and incomplete penetrance are scored as amorphic. Those that did not show a dominant C′ phenotype are considered hypomorphic.

[b] The wing tissue polarity phenotype of homozygotes for the various alleles is compared to *Vang*^{A3} homozygotes. Because *Vang*^{A3} appears to be amorphic (based both on the dominant phenotype and the similar phenotype of *Vang*^{A3}/*Vang*^{A3} and *Vang*^{A3}/*Df* wings), those with a stronger phenotype are scored as antimorphic, those with a similar phenotype are scored as amorphic, and those that cause a weaker phenotype are classified as hypomorphic.

[c] Two different *Df* chromosomes were used. These were *Df*(*2R*)*NP4* and *Df*(*2R*)*w45-30N*.

other alleles the strength of the dominant phenotype did not always predict the strength of the homozygous phenotype. For example, based on the strong dominant C′ phenotype of *Vang*^{A5}/+ wings, we considered *Vang*^{A5} to be an antimorphic allele. However, *Vang*^{A5}/*Df* wings showed a phenotype that appeared weaker than *Vang*^{A3}/*Df*. Thus, we consider this allele to be antimorphic for the dominant C′ phenotype but hypomorphic for the recessive wing hair polarity phenotype. Thus, our data argue that the genetics of *Vang* are complex (further evidence for complexity is found in observations on *Vang*^{4014} described below).

To assess in a quantitative way if *Vang* alleles had a *fz*-like (few multiple hair cells) or *in*-like (many multiple hair cells) cellular phenotype, we determined and plotted the fraction of the dorsal C cell with abnormal hair polarity and the number of multiple hair cells in this region. Previously we found that *fz*-like and *in*-like genes were easily distinguished by this assay (Krasnow and Adler 1994; Adler *et al.* 1998). All except one *Vang* allele fell between the patterns seen for *fz*-like and *in*-like genes as described previously (Figure 2). This included alleles that, on the basis of their dominant phenotypes, are antimorphic (*Vang*^{TBS42}) or amorphic (*Vang*^{A3}). The one *Vang* allele that appeared different from the others (*Vang*^{4014}) fell into the *fz*-like group, as it resulted in very few multiple hair cells although it had a more severe polarity phenotype than any other *Vang* allele (Figure 1F). As a further test that *Vang*^{4014} was a *Vang* allele (and not a mutation in a second gene that interacted with *Vang*), we generated *Vang*^{4014}/*Vang*^{TBS42} females and crossed them to *Vang*^{TBS42}/*CyO* males and examined the progeny for possible wild-type recombinants. None was found among more than 340 straight-winged progeny, consistent with *Vang*^{4014} being an unusual *Vang* allele. We conclude that *Vang* cannot be considered a typical *fz*-like or *in*-like gene with respect to this cellular phenotype. In examining *Vang* wings we observed dramatic local variation in the fraction of multiple hair cells. While local variation in the fraction of multiple hair cells is seen with other tissue polarity mutants, it appeared more extreme for *Vang* than other genes.

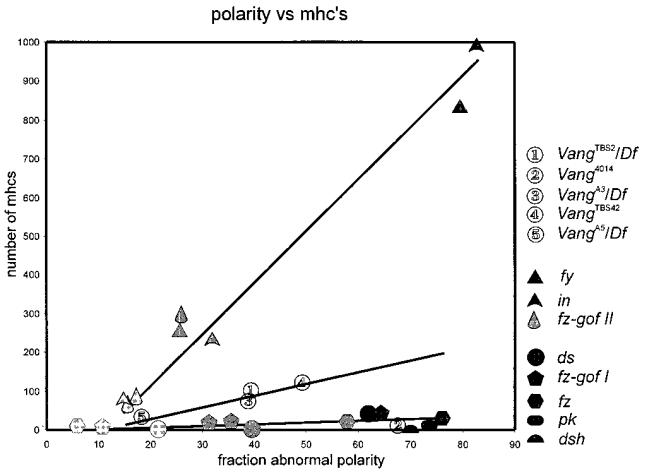

Figure 2.—A plot of the number of multiple hair cells in the dorsal C cell distal to the anterior cross vein as a function of the fraction of this region of the wing that has abnormal polarity. All points except the *Vang* points are taken from Krasnow and Adler (1994) and Adler *et al.* (1998). The darker symbols are stronger alleles and the lightest symbols the weakest alleles of these genotypes. *fz-gofI* stands for the early *fz* gain-of-function phenotype and *fz-gof II* for the late *fz* gain-of-function phenotype (Krasnow and Adler 1994). The five *Vang* genotypes are noted in the figure.

We examined phalloidin-stained *Vang* pupal wings and found that prehairs were formed either in the central regions of the apical surface or at alternative locations along the apical cell periphery of the wing epidermal cells (data not shown). This pattern is typical of the phenotypes of mutations in *fz*-like genes (Wong and Adler 1993).

An alternative scheme for categorizing tissue polarity mutants is the overall abnormal polarity pattern (Adler *et al.* 1998). Mutations in these genes cause stereotypic alterations to hair polarity across the wing. Most tissue polarity mutations fall into the *fz*/*in* polarity group. While mutations in these genes do not produce identical abnormal polarity patterns, there is substantial similarity between the mutant patterns. For example, in all the genes in this group hairs in the D and E cell tend to point toward the wing margin and away from the anterior/posterior compartment boundary. This stands in clear contrast to the unique and quite different patterns seen in *ds* and *pk* mutants (Gubb and Garcia-Bellido 1982; Wong and Adler 1993; Adler *et al.* 1998). By this criteria all ten of our *Vang* alleles fall into the *fz*/*in* polarity group (Figure 3).

Double mutant analysis and gene interactions: We constructed double mutants of *Vang* with *fz*, *dsh* (*dishev-*

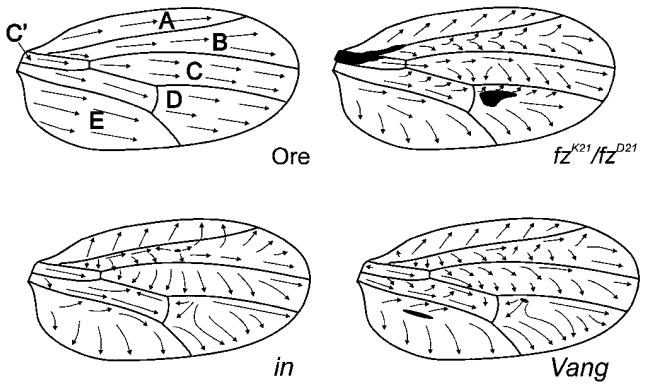

Figure 3.—Shown are drawings of the wing hair polarity pattern on the dorsal surface of a wing of the indicated genotypes. The drawing is of an individual wing, although at least five wings were examined to insure that the drawing represents a typical wing. The A, B, C, D, and E cells of the wing are designated in the Oregon R panel. The filled regions represent regions where neighboring hairs do not show a common polarity (*i.e.*, hair polarity is close to random in these regions).

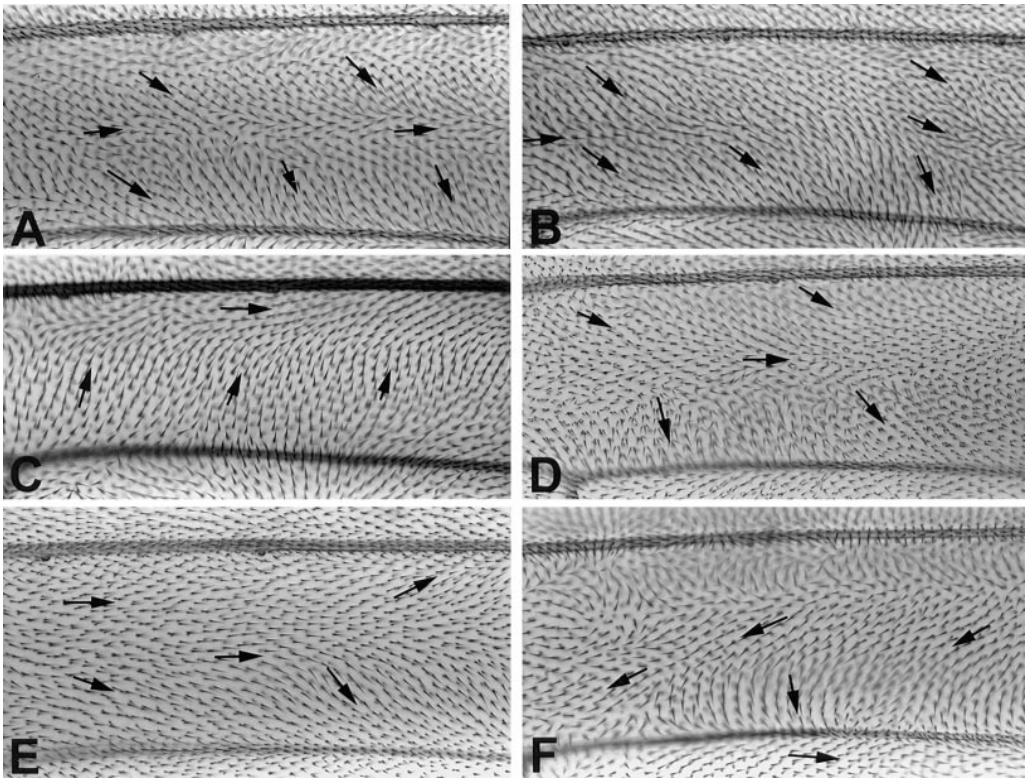

Figure 4.—All micrographs are of the dorsal surface of the wing in the middle C region as in Figure 1. (A) dsh^1/dsh^1; (B) dsh^1/dsh^1; $Vang^{TBS42}/Vang^{TBS42}$; (C) pk^1/pk^1; (D) pk^1 $Vang^{TBS42}/pk^1$ $Vang^{TBS42}$; (E) fz^{R53}/fz^{R53}; and (F) $Vang^{TBS42}/+;fz^{R53}/fz^{R53}$. Note the dsh^1/dsh^1; $Vang^{TBS42}/Vang^{TBS42}$ wing (B) shows the low number of multiple hair cells typical of *dsh* and not the higher number seen in most *Vang* mutants (compare to Figure 1D). The pk^1 $Vang^{TBS42}/pk^1$ $Vang^{TBS42}$ wing has a *Vang*-like polarity pattern and not the *pk* polarity pattern (C *vs.* D and compare to Figure 1D) and an increased number of multiple hair cells. The weak *fz* allele fz^{R53}/fz^{R53} is strongly enhanced by a single dose of $Vang^{TBS42}$ (compare E and F).

elled), *in*, *pk*, and *mwh*. In these experiments we used $Vang^{TBS42}$, $Vang^{A3}$, and $Vang^{A5}$ and obtained similar results with all. The double mutants of *Vang* with *fz*, *dsh*, *in*, and *mwh* all showed the general hair polarity pattern typical of the *fz*/*in* group, to which these genes belong (Figure 4, A and B). The *pk Vang* double mutants also had a *fz*/*in*-like polarity pattern (Figure 4, C and D) (although perhaps less severe than *Vang* single mutants). Thus, by the polarity pattern criterion *Vang* is epistatic to *pk*.

On the basis of casual observation it appeared that the multiple hair cell phenotypes of *dsh*, *in*, and *mwh* were epistatic to *Vang*. We confirmed this by counting the fraction of multiple hair cells in a 20×5 cell region just anterior to the posterior cross vein (Wong and Adler 1993). Thus, all of the strictly cell autonomously acting tissue polarity genes tested appeared to be epistatic to *Vang*. Several strong genetic interactions were seen between *pk* and *Vang* and between *fz* and *Vang*. These are discussed in more detail below.

In other experiments we used the dominant C′ swirl phenotype of *Vang* as a sensitized genetic background to look for dominant interactions of *Vang* and other tissue polarity genes. In these experiments we principally used $Vang^{TBS42}$, as the relatively strong C′ phenotype displayed by this antimorphic allele allowed us to look for enhancement or suppression in a single cross. We did not see any clear-cut interaction between mutations in *dsh*, *in*, *fuzzy* (*fy*), *fritz*, *starry night*, or *mwh* and the *Vang*-dominant phenotype. We also failed to see any interaction between the *Vang*-dominant phenotype and deficiencies for the Wnt-encoding genes *wingless* (*wg*) (and *Wnt4*), *Wnt2*, or *Wnt3*.

The interaction of *Vang* and *pk*: We found that loss-of-function mutations in *prickle* (*pk*) acted as dominant suppressors of the *Vang*-dominant C′ phenotype, suggesting these two genes act in an antagonistic fashion. Several different *pk* alleles (pk^1, pk^{JJ13}, $Df(2R)pk^{78s}$) and several different *Vang* alleles ($Vang^{TBS42}$, $Vang^{14\text{-}11}$, $Vang^{11\text{-}3}$, $Vang^{A3}$) were used, and this interaction was seen in all combinations tested.

pk is a slightly haplo-insufficient gene. A deficiency for *pk* (and some *pk* point mutants) shows a weak, partially penetrant dominant tissue polarity phenotype. This is seen as a swirling of hairs in the D and E cells just distal to the posterior cross vein. Several, but not all, *Vang* alleles acted as enhancers of this haplo-insufficiency of *pk*. For example, $Vang^{A3}$ and $Vang^{TBS42}$, but not $Vang^{11\text{-}3}$, acted as dominant enhancers of the dominant phenotype of $Df(2R)pk^{78s}$. The difference between $Vang^{A3}$ and $Vang^{11\text{-}3}$ is interesting as by other tests both of these alleles were classified as amorphic (Table 1). We also found that *Vang* alleles acted as dominant enhancers of the tissue polarity phenotype seen in flies that carry a single copy of the dominant antimorphic *pk* allele pk^{TBJ21} (R. E. Krasnow and P. N. Adler, unpublished results). These enhancements were unexpected as this interaction is in the opposite direction to the suppression of the *Vang*-dominant C′ phenotype by *pk* mutations. Thus, the interaction between *Vang* and *pk* appears complex.

As noted earlier, double mutants of *pk* and *Vang* showed the *fz*/*in* polarity pattern. Interestingly, the number of multiple hair cells in the *Vang*; *pk* double-mutant wings was increased above that seen in either single mutant (*e.g.*, in our standard test region just anterior to the posterior cross vein we found the following: $Vang^{TBS42}$, 1.39 hairs/cell; pk^{1}, 1.01 hairs/cell; and pk^{1} $Vang^{Tbs42}$, 1.7 hairs/cell). In previous experiments we saw no evidence for any additive or synergistic interactions for this phenotype (Wong and Adler 1993).

The interaction of *Vang* and *fz* is complex: Several different *fz* mutations ($Df(3L)fz^{D21}$; $In(3L)fz^{K21}$, fz^{R52}) were found to act as dominant enhancers of the *Vang*-dominant C′ phenotype associated with $Vang^{TBS42}$ and $Vang^{A5}$. To determine if *Vang* mutations could enhance *fz* mutations we utilized the weak *fz* allele fz^{R53}, which we have previously found to be a sensitive genetic background for detecting genetic interactions (Krasnow *et al.* 1995). We found that *Vang* alleles considered to be either antimorphic or amorphic ($Vang^{TBS42}$ and $Vang^{A3}$) both acted as strong dominant enhancers of fz^{R53} (Figure 4, E and F). From these experiments it appeared that *Vang* and *fz* interacted in a positive fashion.

We constructed and examined the wings of several allelic combinations of *Vang*; *fz* double mutants. In $Vang^{TBS42}$; fz^{1}, $Vang^{A3}$; fz^{1}, $Vang^{A5}$; fz^{1}, $Vang^{TBS42}$; fz^{R54}; $Vang^{A3}$; fz^{R54}/fz^{K21}, and $Vang^{TBS42}$; fz^{K21}/fz^{R54} wings the *fz*/*in* type of polarity pattern was seen, although surprisingly it generally appeared slightly less abnormal than in either single mutant. The number of multiple hair cells was reduced from that seen in the *Vang* single mutants (*e.g.*, $Vang^{A3}$, 1.31 hairs per cell; fz^{R54}, 1.02 hairs per cell; and $Vang^{A3}$;fz^{R54}, 1.13 hairs per cell), although this was rather variable for the $Vang^{TBS42}$; fz^{1} flies both with respect to different individuals and different regions of the wing. Thus, the double mutant studies on *fz* and *Vang*, which gave if anything less severe mutant phenotypes than the single mutants, stand in contrast to those described above where we saw enhancement of mutant phenotypes.

We used Western blot analysis to examine the level of Fz protein in wild-type and *Vang* wing discs. No differences were found, arguing that *Vang* does not regulate *fz* expression.

Vang is not required for the transduction of the *fz* signal: The overexpression of *fz* just before prehair initiation causes the formation of large numbers of multiple hair cells that are a phenocopy of the *in*-like mutations (Krasnow and Adler 1994). This is consistent with our suggestion that a consequence of *fz* signal transduction is the inhibition of the activity of the products of the *inturned*-like genes in the vicinity of the distal vertex (Wong and Adler 1993). Evidence that this *in* phenocopy results from Fz signal transduction antagonizing In/Fy comes from experiments in which we found that the mild overexpression of *fz* (not enough to cause a substantial phenotype by itself) acts as a strong enhancer of weak alleles of *in* and *fy* (R. E. Krasnow and P. N. Adler, unpublished results). We have previously used the ability of *fz* overexpression to phenocopy *in* as a test to identify genes that are downstream of and required for the transduction of the *fz* signal (Krasnow *et al.* 1995). In these experiments we found that the cell autonomously acting *dsh* gene (Klingensmith *et al.* 1994; Theisen *et al.* 1994), but not *pk* or *dachsous*, was required for this phenocopy (Krasnow *et al.* 1995; Adler *et al.* 1998). To determine if *Vang* was required for the transduction of the *fz* signal we constructed *Vang*; *hs-fz* flies and induced *fz* expression just before prehair initiation. We found that the *Vang* mutation did not block the ability of *fz* overexpression to induce cells to form multiple hairs (Table 2). Indeed, if anything it appeared to enhance the ability of *fz* overexpression to induce multiple hair cells.

***Vang* is required for the ability of a gradient of *fz* expression to repolarize wing hairs:** We have found that the induction of a gradient of *fz* expression, with its high point near the distal tip of the wing, results in a reversal of the normal distal polarity of hairs in this region of the wing (Adler *et al.* 1997). Because a similar induction of expression of *dsh* does not produce a region of reversed polarity, it seems likely that polarity reversal requires the cell nonautonomous function of *fz*. In a *dsh* mutant background the induction of a gradient of *fz* expression does not produce a region of reversed polarity; hence, a functional *fz* signal transduction pathway also appears to be needed. To determine if *Vang* function was required for a gradient of *fz* expression to cause a local reversal of wing hair polarity, we induced such a gradient of expression by "distal waxing" of *Vang;hs-fz* pupae (Adler *et al.* 1997). This did not result in a local region of proximal polarity (Table 3); hence, we concluded that *Vang* was required either for the cell nonautonomous function of *fz* or the transduction of the *fz* signal. Because the experiments described above argued that *Vang* was not required for the transduction of the *fz* signal, we were left with the suggestion that *Vang* is required for the cell nonautonomous function of *fz*.

***Vang* acts cell nonautonomously:** In early experiments we found that when we induced unmarked *Vang* clones we saw a tissue polarity phenotype in wings. Thus, it was clear that the *Vang* phenotype would not be completely rescued by neighboring wild-type cells. We generated *Vang koj* clones for two *Vang* alleles ($Vang^{TBS42}$ and $Vang^{A3}$) to determine if clones of *Vang* cells would disrupt the polarity of neighboring wild-type cells as do clones of *fz* (Vinson and Adler 1987; cells homozygous for *koj* produce either no hair or shortened multiple hairs). For both alleles we found that *Vang* clones resulted in regions of surrounding wild-type cells with abnormal polarity (102 of 103 $Vang^{TBS42}$ clones and 108 of 111 $Vang^{A3}$ clones showed the domineering nonautonomy). This domineering nonautonomy was usually

TABLE 2

***Vang* is not required for the transduction of the *frizzled* signal**

Genotype	*Vang*	*Vang*	*Vang;hs-fz*	*Vang;hs-fz*	*hs-fz*	*hs-fz*
Heat shock	No	Yes	No	Yes	No	Yes
Mean number of multiple hair cells (±SD)[a]	76.2 (17.5)	69.8 (27.6)	78.3 (29.5)	244.6 (83.4)	0 (0)	68.6 (38.2)
Number of wings scored	6	8	6	10	8	14
Effect of heat shock	NR	No ($P = 0.85$)[b]	NR	Yes ($P < 0.001$)	NR	Yes ($P = 0.002$)

NR, not relevant.
[a] Mean number of multiple hair cells in the dorsal A region of the wing.
[b] Significance of comparison of genotype with and without heat shock (rank sum test).

seen over less than half of the clone border. In striking contrast to what we have seen with *fz*, the domineering nonautonomy of *Vang* clones was seen in wild-type cells along the proximal (and in part anterior and posterior), but not the distal border of the clone (Figure 5, A–C). Further, the wild-type hairs showing abnormal polarity tended to point away from the clone border, rather than toward it as is seen for *fz* clones (Adler *et al.* 1997).

In these clone experiments we generated not only a *Vang*/*Vang* clone, but also a +/+ twin spot. The cells in this +/+ twin spot might be expected to have a higher level of *Vang* activity than the surrounding *Vang*/+ cells. To determine if these cells influenced the domineering nonautonomy of *Vang* we generated *Vang*^{A3} *koj* and *pwn* twin spots. The *pwn* twin spot cells, which can be recognized because of their thin wispy hairs, would have two copies of the wild-type *Vang* gene and hence potentially higher *Vang* activity than the surrounding cells. We saw no consistent pattern to the location of the *pwn*/*pwn* twin spot as compared to the *Vang koj*/*Vang koj* clone or the domineering nonautonomy (we examined 29 twin spots). Indeed, it was easy to find examples where the twin spot was far removed from the wild-type cells showing the domineering nonautonomy (Figure 5A). Hence, we concluded that the presence of cells with two wild-type *Vang* genes did not play an important role in the domineering nonautonomy of *Vang* clones.

We have carried out a similar twin spot analysis for *fz* (using *fz*^{R52} *strb* and *flr* twin spots) (Figure 5D). Here we also found no consistent pattern to the location of the *fz*^{R52} *strb* and *flr* twin spots (we examined 23 twin spots), leading to the conclusion that the twin spot cells with two doses of *fz* were not important for generating the distal domineering nonautonomy of *fz* (Vinson and Adler 1987).

***Vang* and *fz* mutations suppress the domineering cell nonautonomy of *fz* and *Vang* clones, respectively:** The opposite domineering nonautonomy of *fz* and *Vang* clones, and the genetic interactions described above suggested the possibility that *fz* was involved in the domineering nonautonomy of *Vang* (and vice versa). To determine if *fz* activity was required for the domineering nonautonomy of *Vang* we generated *Vang*^{A3} *koj* clones in a *fz* mutant background. We scored clones for nonautonomy in those regions (*i.e.*, peripheral as opposed to central regions of the wing) where the polarity of hairs in a *fz* mutant was consistent even if abnormal. For example, hairs consistently point toward the margin in the peripheral regions of the D and E cells (see Figure 3). Although *fz* and *Vang* mutations do not produce strong tissue polarity phenotypes in these wing regions, clones in this region that are mutant for either *fz* or *Vang* show strong domineering nonautonomy (Vinson and Adler 1987; Figure 5, A–C). Even in these regions of mutant wings, however, it is more difficult to recognize domineering nonautonomy than in a wild-type

TABLE 3

***Van Gogh* function is required for a gradient of *frizzled* expression to produce a region of reversed wing hair polarity**

Genotype	Number with region of reversed polarity[a]	Number showing other effects of waxing[b]	Number showing no effect of waxing
hs-fz	32	3	10
Vang;hs-fz	0	5	24

[a] Number of wings in the category.
[b] Other effects refer to an induced tissue polarity phenotype other than a region of reversed polarity.

wing, particularly if the effect is not dramatic. This is because the polarity is not as uniform as in a wild-type wing, and the presence of wild-type cells that produce multiple hairs cannot be used as evidence of domineering nonautonomy. Hence, in addition to scoring clones as either positive or negative for a domineering effect as we have in the past, we included the category of weak nonautonomy for clones where there was a hint of domineering nonautonomy, but where the effect was not convincing enough to score it as a clear positive. We scored 21 *Vang*^{A3} clones in *fz*^{R54}/*fz*^{K21} mutant wings. None showed the strong domineering nonautonomy typical of *Vang* clones in an otherwise wild-type wing. Twelve of the 21 clones showed no domineering nonautonomy (Figure 6, A and B) while 9 were classified as producing weak domineering nonautonomy (Figure 6C). In those cases where we saw the weak nonautonomy, it was located proximal to the clone and hairs pointed away from the clone border as is seen for *Vang* clones in a wild-type background. Thus, we conclude that *fz* acts as a suppressor of the domineering nonautonomy of *Vang*.

We also carried out a complementary experiment in which we generated *fz*^{R52} *strb* clones in a *Vang* amorphic mutant background (*Vang*^{A3}). Once again we only scored clones in regions where the polarity of hairs in a *Vang* wing was consistent. We scored 20 clones and found that 15 showed no domineering nonautonomy (Figure 7). The remaining 5 were scored as showing weak domineering nonautonomy. As is the case for *fz* clones in a wild-type wing, these clones affected the polarity of wild-type cells located distal, but not proximal, to the clone. Since more than 85% of *fz* clones typically show clear-cut domineering nonautonomy in a wild-type background (Vinson and Adler 1987; Jones and Adler 1996), *Vang* mutations act as suppressors of the domineering nonautonomy of *fz*.

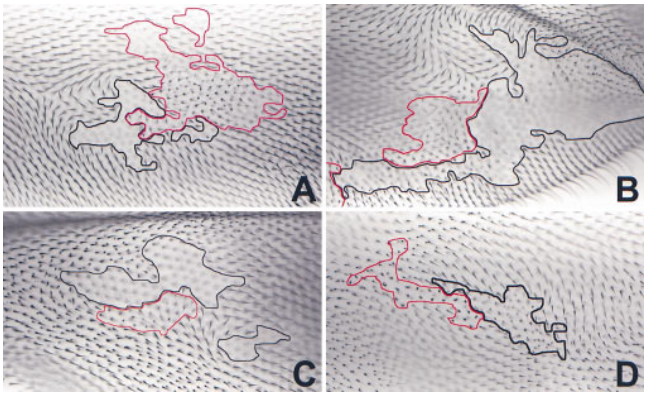

Figure 5.—Domineering cell nonautonomy of *Vang* and *fz* shown in twin spots. A, B, and C show *Vang*^{A3} *koj*^{VB13}/*Vang*^{A3} *koj*^{VB13} clones along with their *pwn* twin spots. The *Vang*^{A3} *koj*^{VB13} clone is outlined in black and the *pwn* clone is shown in red. In A and B, note the wild-type cells proximal to the *Vang*^{A3} *koj*^{VB13} clone that show abnormal polarity. The *pwn* twin spot, which should contain two wild-type copies of *Vang*, is not juxtaposed to the wild-type hairs showing altered polarity. D shows the equivalent experiment showing a *fz*^{R52} *strb*/*fz*^{R52} *strb* clone (outlined in black) and a *flr*/*flr* twin spot (outlined in red). Note the cells distal to the *fz*^{R52} *strb* clone with altered polarity and that the *flr* cells, which should have two doses of *fz*$^{+}$, are not juxtaposed to this region.

DISCUSSION

***Vang* and the *fz* pathway:** The cellular phenotype of *Vang* mutant wings differs from that seen previously for other tissue polarity genes. Most *Vang* alleles result in more multiple hair cells than are seen in a *fz*-like mutant and fewer than are seen in an *in*–like mutant. However, several results suggest that *Vang* is a member of the *fz* signaling/signal transduction pathway. The polarity phenotype of *Vang* mutants is quite similar to that seen in loss-of-function mutations in *fz*, *dsh*, *in*, *fuzzy*, *mwh*, and *fritz*. Thus, on the basis of its polarity phenotype it seems likely that *Vang* mutations inactivate the *fz* pathway. Further, the observation that *dsh*, *in*, and *mwh* are epistatic to *Vang* suggests that *Vang* functions upstream of these genes in the *fz* signaling/signal transduction pathway. Given that it has a phenotype in between that of the *fz*-like and *in*-like genes, a reasonable guess is that it functions between these two groups of genes. However, this is unlikely to be the case. The *dsh* gene, which appears to function between *fz* and *in*, has a *fz*-like mutant phenotype. *dsh* is required for the transduction of the *fz* signal (Krasnow *et al.* 1995) and acts cell autonomously (Klingensmith *et al.* 1994; Theisen *et al.* 1994), as do *in* (Park *et al.* 1996) and *fuzzy* (Collier

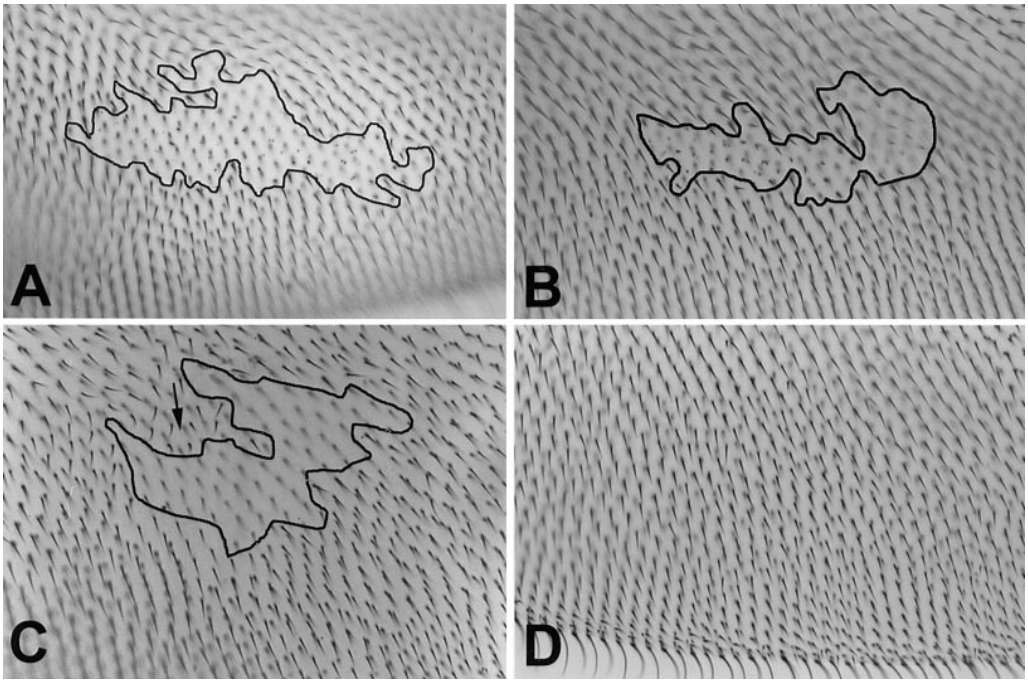

Figure 6.—A, B, and C show *Vang*^{A3} *koj*^{VB13}/*Vang*^{A3} *koj*^{VB13} clones in the E region of *fz*^{R54}/*fz*^{K21} wings. A similar region of a sibling *fz*^{R54}/*fz*^{K21} wing without a clone is shown in D. In A and B the *Vang*^{A3} *koj*^{VB13}/*Vang*^{A3} *koj*^{VB13} clones do not show any evidence of domineering nonautonomy. The clone in C shows an example of what we scored as weak domineering nonautonomy (see region with arrow). Note how this domineering nonautonomy is much less dramatic than is seen for *Vang*^{A3} *koj*^{VB13}/*Vang*^{A3} *koj*^{VB13} clones in a wild-type wing (Figure 5).

and Gubb 1997). In contrast, we found that *Vang* is not required for the transduction of the *fz* signal and acts cell nonautonomously. Hence, *Vang* is unlikely to function downstream of *dsh*. It is possible that *Vang* acts downstream of *fz* (and upstream of *dsh*), but that it is not required for the transduction of the *fz* signal (*e.g.*, it could be a negatively acting factor). However, as is discussed below the data do not suggest a simple quantitative relationship between *fz* and *Vang*. A second possibility is that *Vang* is upstream of both *fz* and *dsh* in the *fz* pathway. Alternatively, there could be two *fz*-dependent pathways (Vinson and Adler 1987; Park *et al.* 1994): a cell autonomous pathway, which includes genes such as *dsh* and *in*, and a cell nonautonomous pathway. The cell nonautonomous pathway would be logically upstream of the cell autonomous pathway and *Vang* could function there.

The nonautonomy of *Vang* and *fz*: Clones mutant for *Vang* showed a remarkable anti-*fz*-like domineering nonautonomy, and this domineering nonautonomy was suppressed in a *fz* mutant background. It is important to note that wild-type hairs whose polarity was affected by a *Vang* clone pointed away from the clone. On the basis of previous data that showed that hairs point from cells of higher Fz levels toward cells of lower levels (Adler *et al.* 1997), it seemed possible that *Vang* mutant cells might have higher than normal *fz* activity (*i.e.*, *Vang* is an inhibitor of *fz* activity). This could also explain the apparent enhancement by a *Vang* mutant background of the ability of late *fz* overexpression to induce an *in-*

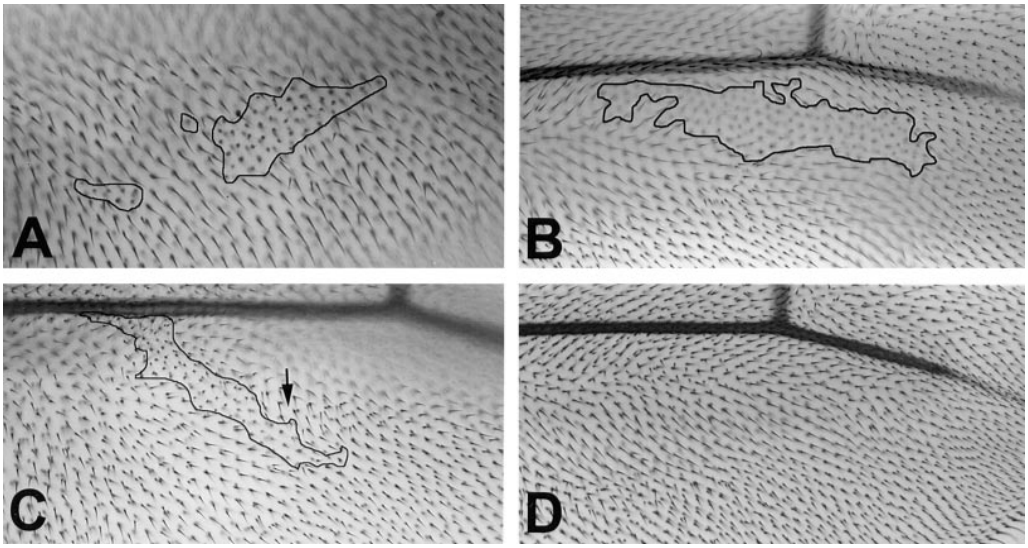

Figure 7.—A, B, and C show *fz*^{R52} *strb*/*fz*^{R52} *strb* clones in the E region of *Vang*^{A3}/*Vang*^{A3} wings. Note the clones in A and B do not appear to alter the polarity of the neighboring cells. C shows an example of weak domineering nonautonomy (see region with arrow). Note how this domineering nonautonomy is much less dramatic than is seen for *fz*^{R52} *strb*/*fz*^{R52} *strb* clones in a wild-type wing (compare to Figure 4D). D shows the equivalent region of a sibling *Vang*^{A3}/*Vang*^{A3} wing without a clone.

like phenotype (see Table 1). However, there are several observations that cannot be explained by this hypothesis. One is that the *Vang* polarity pattern resembles that seen with a loss of function of *fz* or other members of the *fz* signal transduction pathway such as *dsh*. The uniform overexpression of *fz* in the early pupae produces a tissue polarity phenotype, but not one with a polarity pattern whose details resemble the *fz*/*in* polarity pattern (Krasnow and Adler 1994). Thus, the polarity pattern seen in *Vang* mutant wings is not what is expected for an increase in *fz* activity. Further, the ability of *Vang* to dominantly enhance the phenotype of the weak fz^{R53} allele is not expected if *Vang* acts as a negative regulator of *fz* activity. Indeed, if this were the case we would predict that *Vang* mutations should suppress a weak *fz* allele such as fz^{R53}. Similarly, the ability of *fz* loss-of-function mutations to enhance the *Vang*-dominant tissue polarity phenotype is the opposite of what we would expect if *Vang* acted as an inhibitor of *fz* activity. Further, if *Vang* mutations cause a tissue polarity phenotype by increasing *fz* activity, then we would expect that a *fz* gain of function would enhance the *Vang* mutant phenotype. While this may be the case when *fz* is overexpressed just before prehair initiation (as noted above), it was not observed with earlier overexpression (*e.g.*, 12 hours before prehair initiation) or weak overexpression of *fz* (*i.e.*, wild-type gene expression as well as the basal expression of a *hs-fz* gene). Finally, we found that *fz* domineering nonautonomy is suppressed in a *Vang* mutant background. If *Vang* mutations resulted in higher *fz* activity, than the difference in *fz* levels between the *Vang;fz* clone cells and their *Vang;fz*/+ neighbors would be enhanced compared to *fz* clones in a wild-type wing. This seems likely to enhance rather than suppress the domineering nonautonomy of *fz*. Thus, there are data that suggest a positive relationship between *Vang* and *fz*, as well as data that suggest an antagonistic relationship. We conclude that the relationship between *Vang* and *fz* is not simply quantitative.

The extensive genetic interactions seen between *fz* and *Vang*, between *pk* and *Vang*, and between *fz* and *pk* (R. E. Krasnow and P. N. Adler, unpublished results) suggest that these genes are functionally quite close. However, as is discussed in depth earlier for *Vang* and *fz*, the interactions between *Vang* and *pk* and between *fz* and *pk* (R. E. Krasnow and P. N. Adler, unpublished results) also cannot be explained by a simple quantitative interaction. We suggest that the products of these genes may interact physically in a tissue polarity receptor complex, and that interactions at the protein level are responsible for the complex array of interactions detected in our genetic experiments. That the Vang protein might be part of a protein complex is also suggested by the observation that the phenotype of $Vang^{TBS42}$/$Vang^{TBS42}$ wings is stronger than that of $Vang^{TBS42}$/*Df*. This result argues that the antimorphic *Vang* protein produced by this allele is antagonizing the product of another gene, and this is likely to be because of the formation of an inactive protein complex.

Models for tissue polarity and *Vang*: Two types of models have been proposed to account for the role of *fz* in tissue polarity and its domineering cell nonautonomy (Adler *et al.* 1997). One type is typified by the cell-by-cell signaling model, which suggests that each cell becomes polarized because the Fz protein is activated unevenly across cells (Park *et al.* 1994; Adler *et al.* 1997). In one version of this model the binding of Wnt ligand to Fz protein on the proximal side of a cell was suggested to locally inactivate Fz (Figure 8A; Adler *et al.* 1997). Active Fz protein on the distal edge of the cell was suggested to activate several signal transduction pathways. One pathway would lead to prehair initiation at the distal edge of the cell. A second would lead to the release of Wnt ligand at the distal edge of the cell to polarize the next most distal cell. This released Wnt could be newly synthesized or could be molecules transported through the cell, as has been suggested for Wg (Hays *et al.* 1997). The domineering nonautonomy of *fz* would be caused by the failure of the clone cells to release signal. An alternative class of model is represented by the secondary signaling model, which suggests that the Fz protein is differentially activated in cells along the proximal/distal axis of the wing by the nonsaturating binding of a gradient morphogen (Zheng *et al.* 1995; Adler *et al.* 1997). Cells would then produce a secondary signal in amounts that were proportional to the fraction of Fz receptors that bound ligand (Figure 8C). Assessing the level of secondary signal produced by their neighbors would serve to polarize cells. These models differ fundamentally in that *fz* has both cell autonomous and cell nonautonomous functions in the cell-by-cell signaling model while it only has cell nonautonomous functions in the secondary signaling model; and the secondary signal model invokes a long range gradient of a diffusible polarity morphogen. As we have discussed elsewhere, both models have difficulty explaining some data, hence it is not clear which is closer to being correct (Adler *et al.* 1997). As is described below, it is possible to incorporate the data on *Vang* into both of these models.

In the cell-by-cell signaling model *Vang* can be placed into the signal transduction pathway (or transport pathway) that leads to the directional release of the Wnt ligand. To explain the domineering nonautonomy of *Vang* we need to hypothesize that *Vang* mutations result in signal being released in all directions, not just distally (Figure 8B). In this model *Vang* is involved in helping establish the spatial specificity of *fz* action and cannot be thought of as a simple positive or negative factor. This is consistent with the data that do not show a simple quantitative relationship between *fz* and *Vang*. In the absence of *Vang*, *fz* signaling (*i.e.*, release of ligand) would be equivalent in all directions, leading to a lack of polarized cells and a polarity phenotype that is simi-

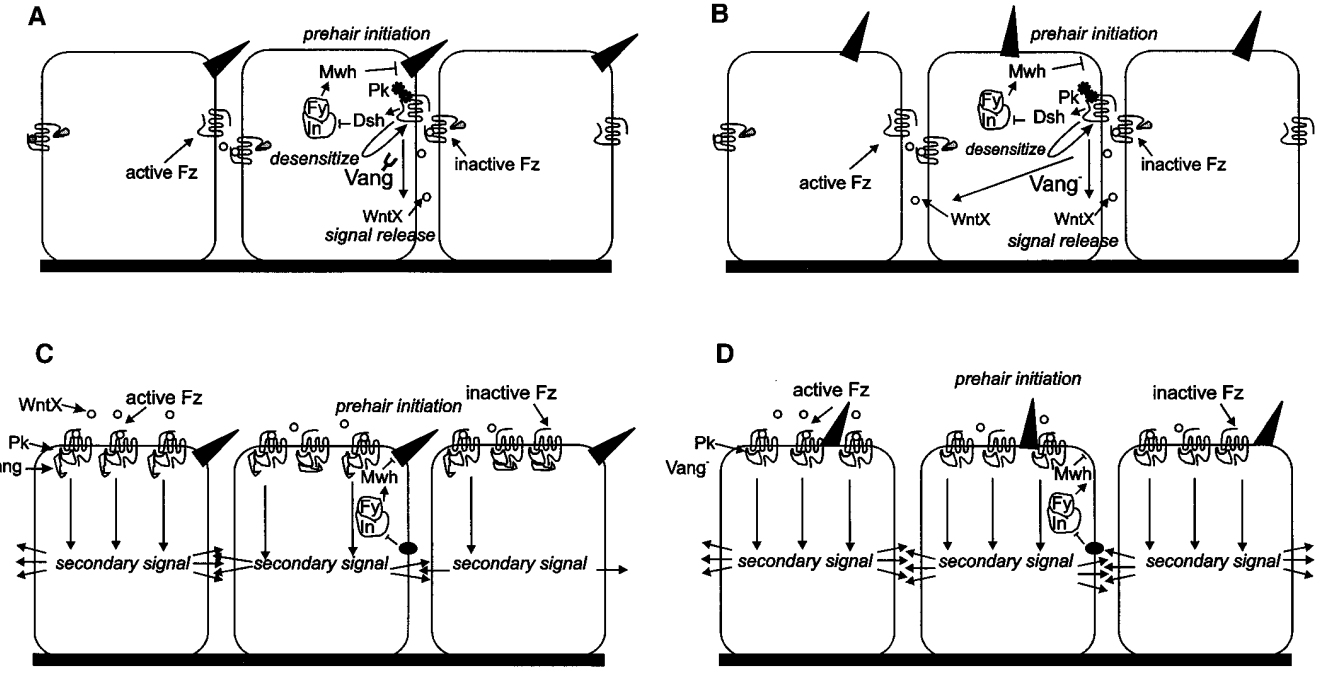

Figure 8.—Shown are models to explain the roles of *fz* and *Vang* in wing tissue polarity. A shows a version of the cell-by-cell signaling model (Adler *et al.* 1997). Wnt ligand released at the distal edge of a cell binds to and inactivates Fz receptor on the proximal edge of neighboring cells. This leads to the activation of *fz*-dependent signal transduction pathways at the distal edge of cells. These signal transduction pathways lead to prehair initiation near the distal vertex resulting in hairs with distal polarity, to the release of Wnt ligand at the distal edge of the cell, and to the desensitization of Fz receptor in the distal part of the cell. The *Vang* gene is hypothesized to be part of the pathway that results in the distal release of *Wnt.* Hence, in a *Vang* mutant Wnt is released proximally as well as distally (B). C shows a version of the secondary signaling model. A gradient of a diffusible morphogen Wnt leads to a gradient of Fz receptor being activated by ligand binding. The activation of Fz receptor leads to the proportional production of a secondary signal. Cells are polarized because of a higher concentration of secondary signal on one side *vs.* the other. The Vang protein is hypothesized to be involved in coupling activated Fz to the production of secondary signal. Thus, in a *Vang* mutant a high constant level of secondary signal is produced (D).

lar to no *fz* signaling. This promiscuous signaling in a *Vang* mutant would be expected to suppress the consequences of the abnormal signaling caused by a *fz* clone, and hence suppress the domineering nonautonomy of *fz.* In the absence of *fz* function the domineering nonautonomy of *Vang* would be suppressed, as this nonautonomy is a consequence of abnormal *fz* signaling. Thus, the cell-by-cell signaling model can incorporate our observations on *Vang.*

In the secondary signaling model we can hypothesize that in a *Vang* mutant a similar high level of secondary signal is produced regardless of the degree of *fz* activation by ligand (Figure 8D). The uniform secondary signal would be equivalent to no secondary signal with respect to polarizing neighboring cells. In such a model *Vang* could be a negative regulator/modulator of *fz* signal transduction. Although it would be downstream of *fz,* as a negative regulator it would not be expected to be required for the transduction of the *fz* signal. This simple model has problems in explaining the interactions noted above that do not suggest a simple quantitative relationship between these two genes; but perhaps these could be explained as a consequence of direct interactions between the proteins.

It is possible that the connection between *fz* and *Vang* is not as close as is suggested above. For example, the activity of these genes could be separated in time. In the developing Drosophila eye it has been suggested that polar/equatorial polarity is established in two phases. The first signal comes from the pole and is dependent on *wingless,* while a later one is hypothesized to originate at the equator and is likely dependent on *fz* (Reifegerste *et al.* 1997; Wherli and Tomlinson 1998). If such a two-phase process functions in establishing wing tissue polarity it is possible that *Vang* could function in the early phase in the establishment of a polarizing signal that later functions in tissue polarity by polarizing *fz* activity. In a *Vang* mutant the polarizing signal could be ubiquitously present, leading to a failure to polarize *fz* activity. *Vang* clones could produce their proximal cell nonautonomy by causing an ectopic source of polarizing signal. The polarizing activity could represent the long-range morphogen hypothesized by the secondary signal model or an initiation center for cell-by-cell signaling.

The mutual suppression of the domineering nonautonomy of *fz* and *Vang* clones by mutations in *Vang* and *fz,* respectively, was not complete. The failure of *Vang*

to completely suppress the domineering nonautomomy of *fz* could be because the *Vang* allele used in these experiments ($Vang^{A3}$) was not a null allele. The further characterization of *Vang* will be required to determine if this is a null allele. We also need to be able to explain the failure of *fz* mutations to completely suppress the domineering nonautonomy of *Vang*. The *fz* genotype used (fz^{R54}/fz^{K21}) in these experiments is expected to produce some protein (fz^{K21}, which is a breakpoint in the first intron of *fz*, is a protein null, but fz^{R54} does produce Fz protein; Jones *et al.* 1996); however, this genotype is a phenotypic null with respect to wing hair polarity. Thus, we think that the failure to see complete suppression is not because of residual *fz* activity. It is possible that partial functional redundancy between *fz* and a second *fz* family member might be responsible for the residual *Vang* nonautonomy. The secondary signaling model can also be modified to account for the residual domineering nonautonomy without invoking any redundancy or mutations not completely inactivating genes. For example, some secondary signal could be produced in the absence of *fz* function and the amount of this signal could be modulated by *Vang*. Thus, clones of *Vang* cells in a *fz* wing could produce more secondary signal than their neighbors and hence still produce some domineering nonautonomy. Similarly, the level of secondary signal produced by clones of *fz* cells in an otherwise *Vang* wing might be less than their neighbors, leading to only partial suppression of the domineering nonautonomy of *fz*.

This work was supported by a grant from the National Institutes of Health (GM37136).

Note added in proof: We have determined that *Van Gogh* is allelic to *strabismus* (Wolff and Rubin, 1998. Development 125: 1149–1159).

LITERATURE CITED

Adler, P. N., 1992 The genetic control of tissue polarity in Drosophila. BioEssays **4:** 735–741.

Adler, P. N., J. Charlton and W. J. Park, 1994 The Drosophila tissue polarity gene *inturned* functions prior to wing hair morphogenesis in the regulation of hair polarity and number. Genetics **137:** 829–836.

Adler, P. N., R. E. Krasnow and J. Liu, 1997 Tissue polarity points from cells of higher toward cells of lower Frizzled levels. Curr. Biol. **7:** 940–949.

Adler, P. N., J. Charlton and J. Liu, 1998 Mutations in the cadherin superfamily gene *dachsous* have a tissue polarity phenotype and affect *frizzled* signaling. Development **125**: 959–968.

Collier, S., and D. Gubb, 1977 Drosophila tissue polarity requires the cell-autonomous activity of the *fuzzy* gene, which encodes a novel transmembrane protein. Development **124:** 4029–4037.

Golic, K. G., and S. Lindquist, 1989 The FLP recombinase of yeast catalyzes site-specific recombination in the Drosophila genome. Cell **59:** 499–509.

Gubb, D., 1993 Genes controlling cellular polarity in Drosophila. Development (Suppl.): 269–277.

Gubb, D., and A. Garcia-Bellido, 1982 A genetic analysis of the determination of cuticular polarity during development in Drosophila melanogaster. J. Embryol. Exp. Morphol. **68:** 37–57.

Hays, R., G. B. Gibori and A. Bejsovec, 1997 Wingless signaling generates pattern through two distinct mechanisms. Development **124:** 3727–3736.

Held, L. I., C. M. Duarte and K. Derakhshanian, 1986 Extra tarsal joints and abnormal cuticular polarities in various mutants of *Drosophila melanogaster*. Roux's Arch. Dev. Biol. **195:** 145–157.

Jones, K. H., J. Liu and P. N. Adler, 1996 Molecular analysis of EMS induced *frizzled* mutations in *Drosophila melanogaster*. Genetics **142:** 205–215.

Klingensmith, J., R. Nusse and N. Perrimon, 1994 The Drosophila segment polarity gene *dishevelled* encodes a novel protein required for response to the *wingless* signal. Genes Dev. **8:** 118–130.

Kopp, A., and I. Duncan, 1997 Control of cell fate and polarity in the adult abdominal segments by *optomoter-blind*. Development **124:** 3715–3724.

Krasnow, R. E., and P. N. Adler, 1994 A single frizzled protein has a dual function in tissue polarity. Development **120:** 1883–1893.

Krasnow, R. E., L. L. Wong and P. N. Adler, 1995 *dishevelled* is a component of the *frizzled* signaling pathway in *Drosophila*. Development **121:** 4095–4102.

Park, W. J., J. Liu and P. N. Adler, 1994 The *frizzled* gene of Drosophila encodes a membrane protein with an odd number of transmembrane domains. Mech. Dev. **45:** 127–137.

Park, W. J., J. Liu and P. N. Adler, 1996 The Drosophila tissue polarity gene *inturned* acts cell autonomously and encodes a novel protein. Development **122:** 961–969.

Reifegerste, R., C. Ma and K. Moses, 1997 A polarity field is established early in the development of the Drosophila compound eye. Mech. Dev. **68:** 69–79.

Struhl, G., D. A. Barbash and P. A. Lawrence, 1997 Hedgehog acts by distinct gradient and signal relay mechanisms to organize cell type and polarity in the Drosophila abdomen. Development **124:** 2155–2165.

Strutt, D. I., U. Weber and M. Mlodzik, 1997 The role of RhoA in tissue polarity and Frizzled signaling. Nature **387:** 292–295.

Theisen, J., J. Purcell, M. Bennett, D. Kansagara, A. Syed *et al.*, 1994 *Dishevelled* is required during wingless signaling to establish both cell polarity and cell identity. Development **120:** 347–360.

Vinson, C., and P. N. Adler, 1987 Directional non-cell autonomy and the transmission of polarity information by the *frizzled* gene of *Drosophila*. Nature **329:** 549–551.

Wherli, M., and A. Tomlinson, 1998 Independent regulation of anterior/posterior and equatorial/polar polarity in the Drosophila eye. Development **125:** 1421–1432.

Wong, L. L., and P. N. Adler, 1993 Tissue polarity genes of Drosophila regulate the subcellular location for prehair initiation in pupal wing cell. J. Cell Biol. **123:** 209–221.

Xu, T., and G. M. Rubin, 1993 Analysis of genetic mosaics in developing and adult Drosophila tissues. Development **117:** 1223–1237.

Zheng, L., J. Zhang and R. Carthew, 1995 *frizzled* regulates pattern formation in the Drosophila eye. Development **121**: 3045–3055.

Communicating editor: T. Schüpbach